Comparative study on ATR-FTIR calibration models for monitoring solution concentration in cooling crystallization

Fangkun Zhang[†], Tao Liu [†*], Xue Z. Wang[‡], Jingxiang Liu[†], Xiaobin Jiang[§]

[†] Institute of Advanced Control Technology, Dalian University of Technology, Dalian, 116024, P. R. China,

[‡] School of Chemical and Process Engineering, University of Leeds, Leeds LS2 9JT, UK.

[§] State Key Laboratory of Fine Chemicals, R&D Center of Membrane Science and Technology, School of Chemical Engineering, Dalian University of Technology, Dalian, 116024, P. R. China

[*] Corresponding author. Tel: +86-411-84706465; Fax: +86-411-84706706

Abstract: In this paper calibration model building based on using an ATR-FTIR spectroscopy is investigated for in-situ measurement of the solution concentration during a cooling crystallization process. The cooling crystallization of L-glutamic Acid (LGA) as a case is studied here. It was found that using the metastable zone (MSZ) data for model calibration can contribute to the prediction accuracy, compared to the usage of undersaturated zone (USZ) spectra as traditionally practiced which may lead to undesired bias for prediction of the MSZ concentration. Calibration experiments were made for LGA solution under different concentrations. Four candidate calibration models were established using different zone data for comparison, based on a multivariate partial least-squares (PLS) regression algorithm for the collected spectra together with the corresponding temperature values. Experiments under varied concentrations and operational changes of temperature were conducted. The results indicate that using MSZ spectra for model calibration can give more accurate prediction of the solution concentration during the crystallization process. The primary reason was clarified as spectral nonlinearity for measurement between USZ and MSZ. In addition, an LGA cooling crystallization experiment was performed to verify the sensitivity of these calibration models for monitoring the crystal growth process.

Keywords: Solution concentration, cooling crystallization, ATR-FTIR spectra, model calibration, metastable zone, L-glutamic acid.

1. Introduction

Supersaturation is the decisive driving force with respect to the kinetics of crystallization. Accurate measurement of supersaturation (or solution concentration) is a prerequisite in process for the real-time control of crystals with a desired size, shape, and purity. Since a densitometer was proposed to measure solution concentration in real time by Garside and Mullin [1], a few techniques based on using the refractive index [2], densitometry [3], conductometry [4], or calorimetry [5] had been developed for measuring the solution concentration. Due to the limits of industrial sensors and working conditions, e.g. measurement of conductivity is not available for the majority of organic solvents, the above mentioned techniques have not been widely applied for industrial crystallization monitoring and control [6, 7]. With the rapid development of spectroscopy technology, the corresponding instruments for in-situ/online measurement have been developed for crystallization process monitoring, including attenuated total reflectance Fourier transform infrared spectroscopy (ATR-FTIR), near infrared (NIR) spectroscopy, and ATR-UV/vis. Among these instruments, ATR-FTIR is increasingly applied for various crystallization processes [8], owing to the fact that it is scarcely affected by the particles suspended in the crystallization solution.

For using ATR-FTIR spectroscopy to measure the solution concentration, a key step is to build the calibration model, which requires proper design of experiments (DoE) to collect ATR-FTIR spectra for model calibration. In fact, experiments for ATR-FTIR calibration had been mainly carried out in the undersaturated zone (USZ) [9-15]. A small number of calibration methods were presented in the literature to analyze ATR-FTIR spectra for in-situ measurement of the solution concentration. Lewiner et al. [9] proposed a calibration procedure with undersaturated conditions for three solute/solvent systems, obtaining temperature-dependent models which showed the averaged relative prediction errors no less than 2%. Liotta et al. [10] adopted an amount of ATR-FTIR spectra collected in USZ to build a partial least-squares (PLS) calibration model for predicting the concentration of an active pharmaceutical ingredient (API) during crystallization, resulting in the averaged relative prediction error about 2.9%. For monitoring the cooling crystallization process of L-glutamic acid (LGA), a PLS calibration model of the solution

concentration was built based on the ATR-FTIR spectra collected in USZ [11], giving the averaged relative prediction error about 6.9%. Chen et al. [12] developed an extended loading space standardization method to enhance the model prediction based on the above type spectra for LGA solution, which reduced the relative prediction error to 0.7%~2.5%. The recent references [13, 15] presented rapid PLS-based calibration methods based on the USZ spectra for real-time measurement of the ammonium sulphate and urea crystallization processes, respectively. By comparison, only a few references [16-19] suggested that the metastable zone (MSZ) spectra should be taken into account for model calibration because the crystallization process is mainly operated in MSZ. It was proposed [16, 17] to combine the USZ spectra with the MSZ spectra for calibration to improve prediction accuracy on the solution concentration of potassium dihydrogen phosphate (KDP) and LGA during crystallization, therefore reducing the averaged prediction error to 0.37 g/L solvent for LGA solution. Cornel et al. [18] used the collected USZ and MSZ spectra together to build a calibration model in terms of the PCR and PLSR algorithms for LGA solution, indicating smaller root mean square error of cross validation (RMSECV) by using PLSR, i.e. 0.186 g/kg solvent. Zhou et al. [19] also used the USZ and MSZ spectra to build a calibration model for predicting the solution concentration during cooling or anti-solvent crystallization.

Note that in a cooling crystallization process, the operating window of MSZ should be accurately measured for monitoring and control of the crystal nucleation and growth. It is therefore necessary to perform experiments to collect the MSZ spectra for model calibration. To study the model prediction accuracy, different calibration models are established in this paper for comparison by using MSZ spectra, USZ spectra, and a combination of MSZ and USZ spectra, respectively. The validity and prediction accuracy of these established models are verified via experiments for LGA solution. Based on analyzing the prediction errors, it is demonstrated that using the MSZ spectra for calibration can surely obtain good prediction accuracy in the crystallization window, while the combination of MSZ and USZ spectra for calibration compromises the prediction accuracy for both MSZ and USZ owing to the spectral nonlinearity for concentration measurement in these zones. Besides, a cooling crystallization experiment was performed to verify the sensitivity of these calibration models for monitoring the crystal growth process.

2. Experiments

2.1 Materials

To study the calibration problem for in-situ measurement of a crystallization solution, the material of LGA (chemical formula: $C_5H_9NO_4$, β-form, molecular weight: 147.13 g/mol, purity: 99%, product of Sigma) and distilled water were used for experiment. LGA has two recognized polymorphic forms: the metastable, more soluble and prismaticα-form, and the stable, less soluble and needle-like β-form [20]. A high-resolution analytical balance (made by Mettler-Toledo) with precision of one ten thousandth was used to weigh the LGA samples for experiment.

2.2 Experimental set-up

Experimental set-up was shown in Figure 1, consisting of a 4 L jacketed glass crystallizer, a thermostatic circulator (Julabo-CF41), a Pt100 temperature probe, and a PTFE 4-paddle agitator. The stirring speed was maintained at 150 r/min for all experiments. A diamond ATR immersion probe connected via AgX Fiber as the internal reflectance element attached to the FTIR spectrophotometer with MCT Detector was used to collect the absorbance spectra of LGA solution. The ATR-FTIR spectra were collected by a commercial software named ReactIR15 made by Mettler-Toledo Company.

A noninvasive imaging system including two high-resolution cameras made by Hainan Six Sigma Intelligent Systems Ltd. (product no. Stereo Vision Crystal-G) was used to detect crystal nucleation during the cooling process. Both cameras were fixed at a pre-defined angle outside the crystallizer jacket for snapshot as tested in the references [21, 22]. The cameras (UI-2280SE-C-HQ) with CCD sensors and USB Video Class standard were made by IDS Imaging Development Systems GmbH, which can take maximum 6.5 images per second with the pixel resolution of 2448×2050.

2.3 Data collection for calibration

Figure 2 shows the solution concentrations (9.0, 15.0, 21.0, 27.0, 33.0, 39.0 g/L) and the temperature range (15-75 °C) tested for calibrating the LGA aqueous solution. Four subplots in

Figure 2 show the sampled spectra for building 4 candidate models for comparison. Before performing each experiment, the crystallizer and all the detecting probes were cleaned thoroughly by distilled water to avoid impurities or residues. The initial solution (9.0 g/L) was prepared using the above LGA material and 2 L distilled water in the 4 L crystallizer, stirred by a PTFE 4-Paddle agitator at a speed of 150 rpm. For each experiment, the solution was first heated up to 75 °C and the temperature was maintained for 90 minutes to guarantee complete dissolution of the added LGA crystals. Then the solution was cooled down to 15 °C at a fast cooling rate of 0.8 °C/min. The ATR-FTIR spectra and solution temperature were sampled with respect to the time during the cooling process until the occurrence of crystal nuclei as detected by the above imaging system. After that, the solution was reheated up to 75 °C, LGA crystals were further added into the crystallizer to have a higher solution concentration. The temperature was again maintained for 90 minutes to guarantee complete dissolution of LGA crystals. Then the ATR-FTIR spectra and solution temperature were sampled by cooling down the solution to 15 °C at a fast cooling rate of 0.8 °C/min. The above procedure was repeated until all the solution concentrations had been tested. The whole experiment was carried out under the room temperature and repeated to collect the ATR-FTIR spectra and solution temperature for three batches of cool crystallization. The supersaturation curve with respect to a cooling rate of 0.2 °C/min is plotted as the dashed gray line in Figure 2. Data collection is therefore made to cover the undersaturated, saturated, and supersaturated/metastable zone (the operating window for crystallization), in order to build candidate models for comparison.

Note that the metastable zone width (MSZW) is a function of cooling rate, a faster cooling rate generating a wider MSZW [23, 24]. To guarantee no nucleation during in-situ measurement tests for precise calibration, the infrared (IR) spectra were quickly sampled at a fast cooling rate of 0.8 °C/min for all experiments. Spectral data were collected in a range from 650 cm^{-1} to 3000 cm^{-1}, based on an average over 64 scans using 8 wavenumber resolution. The background scan was conducted in air at the room temperature for data collection. All IR spectra were recorded using the ReactIR15 data acquisition software package named iC Quant.

For comparison, four candidate calibration models are established based on using different zones data as shown in Figure 2, i.e.

(1) Overall Model (marked as M1), by using all spectral data sampled from USZ and MSZ.

(2) Cross-zone Model (marked as M2), by using the spectra data sampled from MSZ and a part of spectra data from USZ just below the solubility curve (with a temperature difference smaller than 10 °C) of β-form LGA solution.

(3) MSZ Model (marked as M3), by using the spectral data purely sampled from MSZ.

(4) USZ Model (marked as M4), by using the spectral data purely sampled from USZ.

For each of the above sample solution concentrations, three separate experiments are performed in terms of the same measurement conditions. The IR spectra data collected for calibration are evenly divided into two sets, i.e. almost 75% data used as the training set for calibration and the rest data as the test set for verification. Table 1 lists the number of sampled data from these three experiments to build the above four calibration models, respectively.

3. Calibration model building

To establish a calibration model, it is necessary to determine a suitable range of IR spectra for model fitting with respect to the solution concentration. For the LGA solute, the characteristic absorption bands of the molecular functional groups were marked from the wavenumber 1730 cm^{-1} to 1410 cm^{-1} by Schöll et al [25], which are summarized in Table 2 for reference. Figure 3 (a) shows a number of representative absorption spectra collected by ATR-FTIR spectroscopy at different LGA solution concentrations. These spectra are shown in the wavenumber range from 1500 cm^{-1} to 1100 cm^{-1} based on a baseline correction at the wavenumber 1376 cm^{-1}, for a clear view of the spectra characteristics. In Figure 3 (a), the spectra cover the solution concentration range from 9.0 g/L to 39.0 g/L with respect to the same temperature of 46 °C. Two distinct absorption bands were observed in the wavenumber ranges of 1230-1215 cm^{-1} and 1430-1380 cm^{-1}, respectively. Note that the characteristic peak at the wavenumber 1406 cm^{-1} arises from the symmetric stretching vibration of the carboxyl group, and another peak in the range of 1230-1215 cm^{-1} arises from the stretching vibration of the C-O bond. Figure 3(b) plots the linear relationship between the absorbance peak and the solution concentration at the wavenumbers of 1406 cm^{-1} and 1219 cm^{-1} with respect to the same temperature (46 °C) for measurement, respectively. It indicates that the

solution concentration can be effectively calibrated by the absorbance peak with respect to the same temperature, as adopted in the existing references (e.g. [26, 27]). However, using a univariate peak-ratio method for calibration cannot guarantee measurement accuracy when there exist variations in the solution temperature and environmental conditions for measurement. Figure 4 shows the spectra collected at the solution concentration of 27.0 g/L with respect to a temperature range from 27 °C to 65 °C. Note that the characteristic absorption peak at the wavenumber 1219 cm^{-1} increases with the temperature rising, while the absorption peak at the wavenumber 1406 cm^{-1} decreases with the temperature rising. At the meantime, it is seen that there exists a shift of absorption peaks, e.g. those of the wavenumbers 1406 cm^{-1} and 1219 cm^{-1}. The fact implies a nonlinear relationship between the absorption peaks in the wavenumber range with respect to the temperature change. It is therefore verified that the temperature has a considerable influence to the measurement of IR spectra, which should be taken into account for model calibration as pointed out in the reference [17]. The fact also explains why the classical univariate peak-ratio method cannot provide good measurement accuracy on the solution concentration when the temperature changes during a crystallization process.

Due to the low solubility of LGA aqueous solution and the protonation of the distal carboxylic acid group, the characteristic absorption bands of LGA are less obvious than those of water and sensitive to environmental disturbance and measurement noise [12]. To ensure the calibration accuracy and validity against environmental variation or disturbance, it is preferred to use the IR spectra in a broad wavenumber range that covers the main absorption peaks of LGA functional groups for model calibration, i.e. the wavenumber range of 1800-1000 cm^{-1}, based on experimental tests. Therefore, the following model structure is adopted for calibrating the LGA solution concentration,

$$c = \sum_{j=1000}^{1800} b_j a_j + b_T T \tag{1}$$

where c is the solution concentration in [g/L], a_j is the absorbance, T is the celsius temperature, b_j and b_T are model coefficients.

Based on above analysis and the proposed model structure in (1), a multivariate PLS

regression algorithm is used to build the above candidate calibration models.

4. Results and discussions

4.1 Model validity

To assess the validity of the established models based on using different zone spectra as aforementioned, three commonly used criteria are adopted, i.e. the correlation coefficient (R^2), root-mean-square error of calibration (RMSEC) and root-mean-square error of prediction (RMSEP). Note that RMSEP is computed to measure the accuracy of model prediction regarding the test data that are not used for establishing these models.

Table 3 lists the fitting results of all the established calibration models (M1, M2, M3, M4). It is seen that all of these calibration models results in good agreement on R^2, over 99% for both the training and test sets, well demonstrating the validity of the proposed PLS modeling. Note that both the RMSEC and RMSEP criteria are close to each other for these calibration models, indicating good accuracy for both fitting and prediction with respect to the test data.

Figure 5 shows the model coefficients of M3 and the IR spectrum for the LGA solution concentration 15.0 g/L collected at temperature 25 °C. It is seen that the contribution of each model coefficient is coherent with the corresponding absorption peaks of IR spectrum and LGA functional groups shown in Table 2. A positive coefficient value indicates a positive correlation between the absorption peak at a specific wavenumber and the solution concentration as illustrated in Figure 3(a), and vice versa. It is obvious to conclude that the spectral data in the wavenumber range from 1800 to 1000 cm^{-1} contribute dominantly to the calibration model. The largest contribution comes from a neighborhood of the wavenumber 1730 cm^{-1} due to the stretching vibration of C=O. In addition, the value of temperature coefficient is also plotted in Figure 5. It is seen that the temperature coefficient has a significant effect on the calibration model, which is in accordance with the results shown in Figure 4. It is therefore demonstrated that the temperature is an important factor that should be taken into account for model calibration.

4.2 Model prediction experiments

Experiments for verifying the validity of the established calibration models were performed by in-situ measuring the cooling process of LGA solution for crystallization. Three LGA solution concentrations were tested, i.e. 12.0 g/L, 23.0 g/L, 35.0 g/L, different from the above sample concentrations for calibration. For each test, the solution was first heated up to 75 °C or 85 °C and the temperature was maintained for more than two hours to guarantee complete dissolution of LGA crystals. Then the solution was cooled down to 15 °C at the cooling rate of 0.8 °C/min. The spectra and temperature data were sampled with respect to the time, while the established calibration models were used for real-time monitoring of the solution concentration. The aforementioned imaging system was employed to detect if crystal nuclei occur during the cooling process.

Table 4 lists the prediction results of four calibration models for these three solution concentrations. For each model, the mean prediction value based on the collected spectra is shown along with the averaged relative prediction error (%) for monitoring USZ and MSZ, respectively. The best results are highlighted by bold numbers. It is seen that for monitoring MSZ, the best prediction is given by M3, while notable prediction error is given by using M4. In fact, MSZ is key important for monitoring the crystallization process, where accurate measurement of the solution concentration (relating to the supersaturation level) is vital for the control of crystal nucleation and growth. For monitoring USZ, it is reasonable to see that M4 gives the best prediction result owing to purely using the IR spectra sampled in USZ for model building. Note that M2 gives relatively larger prediction error for monitoring USZ. The reason lies with the fact the PLS modeling based on a finite number of sampled data cannot well describe the nonlinear relationship between cross-zone spectra, which inevitably sacrifices the calibration accuracy for either USZ or MSZ. The spectral nonlinearity may be provoked by the following factors:

(1) Temperature is a salient factor causing the spectral nonlinearity. It has been shown in Figure 4 that there exists shifts of IR spectra along the wavenumber axis with respect to the temperature change, given the same solution concentration of 27.0 g/L. Moreover, Figure 6 shows the absorption peaks (at the wavenumbers 1406 cm^{-1} and 1219 cm^{-1}) with respect the temperature change for measuring three different solution concentrations (15 g/L, 21 g/L, 27 g/L). It is

obviously seen that the absorption peaks have nonlinear variation under the temperature change, given the same solution concentration for measurement.

(2) The chemical unit is another potential factor likely causing the spectral nonlinearity. According to the Beer-Lambert law, absorbance is linearly related to the molarity of solute in the solution at a constant temperature. However, the percentage of solute mass over solvent mass, or solute mass over solvent volume, was commonly used as the unit of concentration instead of molarity for analysis of crystallization processes, as addressed in the references [12]. In fact, the relationship between molarity and the above percentage is nonlinear. If the solution concentration is customarily expressed in terms of the above percentage, the linear relationship between the spectral absorbance and the solution concentration will be distorted.

(3) Measurement uncertainty associated with ATR-FTIR spectroscopy such as the optical fiber tortuosity and spectral shift relating to the environmental conditions, can also give rise to the spectral nonlinearity. Such influence cannot be overlooked in practice, in particular for the case that the target component corresponds to low spectral intensity compared to that of the solution or background for measurement.

Note that although advanced linear or nonlinear modelling algorithms may be explored to deal with the spectral nonlinearity, as discussed in the reference [12, 28], Table 4 indicates that using a piecewise modeling strategy for USZ and MSZ can easily improve the measurement accuracy. Specifically, M3 and M4 give more accurate prediction for MSZ and USZ, respectively. In contrast, M1 gives compromised prediction accuracy for monitoring both MSZ and USZ, based on using all spectra sampled in MSZ and USZ for the model building.

In addition, it is seen from Table 4 that all the averaged relative prediction errors of these calibration models are reduced with the increment of the solution concentration, indicating that better prediction accuracy is obtained for a higher solution concentration by all of these models. This may be owing to the fact that the IR spectra sampled at a higher solution concentration have a higher signal-to-noise ratio than those sampled at a lower solution concentration.

Figure 7 shows the real-time prediction results of four calibration models for the above solution concentrations. It is seen that for initially monitoring USZ (on the left of the dash line),

M1 and M4 give better prediction accuracy than M2 and M3, owing to the use of USZ spectra for calibration. Subsequently, for monitoring MSZ (on the right of the dash line), M3 gives the best prediction accuracy, while M4 shows apparent prediction errors. The results further demonstrate that building piecewise calibration models based on IR spectra sampled in USZ and MSZ, respectively, can guarantee the prediction accuracy.

4.3 Monitoring experiment on the crystallization process

An unseeded cooling crystallization experiment was carried out to test the performance of the established calibration models for monitoring the crystallization process of LGA solution. The initial solution concentration and temperature was 35.0 g/L and 85 °C, respectively. The same cooling experiment was performed as above while all the established calibration models were employed for monitoring the cooling crystallization process in real time. The aforementioned imaging instrument was employed to detect crystal nucleation.

Figure 8 shows the prediction results of these calibration models together with the image results taken at a few representative moments of 28 min, 44 min, 62 min and 83 min. It is seen that M1 and M4 give good prediction of the solution concentration for USZ (roughly before 28 min), and M1, M2, M3 give good prediction for MSZ (roughly from 28 min to 83 min) with reference to the imaged photos. Note that the imaging system detects the crystal nucleation at 44 min as shown in Figure 8, while all the established calibration models give no indication of the concentration change. This demonstrates that the ATR-FTIR spectroscopy is incapable of monitoring crystal nucleation, owing to the fact that the occurrence of crystal nuclei does not lead to a notable change of solution concentration that can be detected by using the established calibration models. Also note that there appears a sharp decrease of the solution concentration predicted by all the established models, when an amount of crystal nuclei are turned out from the solution as verified by the imaging photo taken at the time of 83 min. The rapid change of the solution concentration after 83 min as predicted by the established models indicates that these models may be used for predicting the occurrence of drastic crystal nucleation and monitoring the crystal growth process.

5. Conclusions

For in-situ measurement of solution concentration in cooling crystallization using the ATR-FTIR spectroscopy, calibration model building has been investigated in this paper based on experiments for LGA solution. Four candidate models, named M1, M2, M3, M4, were established by using IR spectra sampled from USZ and MSZ, respectively, for comparing measurement accuracy. It has been revealed that using MSZ spectra to establish a calibration model (M3) shows good prediction accuracy on the solution concentration for monitoring the operating window of cooling crystallization. In contrast, using USZ spectra for model calibration (M1) as mostly adopted in the literature could yield undesired prediction error for MSZ that is mainly concerned for crystallization, due to the spectral nonlinearity as clarified herein regarding the temperature change and chemical unit etc for measurement. It is therefore proposed to build piecewise calibration models to ensure prediction accuracy for MSZ and USZ, respectively. Moreover, it is found by the contribution of the PLS model coefficients that the solution temperature has an important effect for building the calibration model, which should be definitely taken into account for in-situ measurement of solution concentration in cooling crystallization. In addition, it is found by an LGA crystallization experiment that the established calibration models for using the ATR-FTIR spectroscopy are not sensitive to detect the occurrence of crystal nuclei compared to an imaging monitoring system, but can be effectively used for predicting the occurrence of drastic crystal nucleation.

References

[1] J. Garside, J. Mullin, Continuous measurement of solution concentration in a crystalliser, Chem Ind-London, (1966) 2007.

[2] J.E. Helt, M.A. Larson, Effects of temperature on the crystallization of potassium nitrate by direct measurement of supersaturation, AIChE Journal, 23 (1977) 822-830.

[3] S.M. Miller, J.B. Rawlings, Model identification and control strategies for batch cooling crystallizers, AIChE Journal, 40 (1994) 1312-1327.

[4] M.W. Hermanto, A. Phua, P.S. Chow, R.B. Tan, Improved C-control of crystallization with reduced calibration effort via conductometry, Chemical Engineering Science, 97 (2013) 126-138.

[5] O. Monnier, G. Fevotte, C. Hoff, J. Klein, Model identification of batch cooling crystallizations through calorimetry and image analysis, Chemical Engineering Science, 52 (1997) 1125-1139.

[6] Z.Q. Yu, J.W. Chew, P.S. Chow, R.B.H. Tan, Recent advances in crystallization control an industrial perspective, Chemical Engineering Research and Design, 85 (2007) 893-905.

[7] S.S. Kadam, E. van der Windt, P.J. Daudey, H.J.M. Kramer, A comparative study of ATR-FTIR and FT-NIR spectroscopy for in-situ concentration monitoring during batch cooling crystallization processes, Crystal Growth & Design, 10 (2010) 2629-2640.

[8] Z.K. Nagy, R.D. Braatz, Advances and new directions in crystallization control, Annual Review of Chemical and Biomolecular Engineering, 3 (2012) 55-75.

[9] F. Lewiner, J.P. Klein, F. Puel, G. Fevotte, On-line ATR FTIR measurement of supersaturation during solution crystallization processes. Calibration and applications on three solute/solvent systems, Chemical Engineering Science, 56 (2001) 2069-2084.

[10] V. Liotta, V. Sabesan, Monitoring and feedback control of supersaturation using ATR-FTIR to produce an active pharmaceutical ingredient of a desired crystal size, Organic Process Research & Development, 8 (2004) 488-494.

[11] A. Borissova, S. Khan, T. Mahmud, K.J. Roberts, J. Andrews, P. Dallin, Z.P. Chen, J. Morris, In situ measurement of solution concentration during the batch cooling crystallization of L-glutamic acid using ATR-FTIR spectroscopy coupled with chemometrics, Crystal Growth

& Design, 9 (2009) 692-706.

[12] Z.P. Chen, J. Morris, A. Borissova, S. Khan, T. Mahmud, R. Penchev, K.J. Roberts, On-line monitoring of batch cooling crystallization of organic compounds using ATR-FTIR spectroscopy coupled with an advanced calibration method, Chemometrics and Intelligent Laboratory Systems, 96 (2009) 49-58.

[13] S.S. Kadam, A. Mesbah, E. van der Windt, H.J.M. Kramer, Rapid online calibration for ATR-FTIR spectroscopy during batch crystallization of ammonium sulphate in a semi-industrial scale crystallizer, Chemical Engineering Research and Design, 89 (2011) 995-1005.

[14] N. Gherras, G. Fevotte, Comparison between approaches for the experimental determination of metastable zone width: A case study of the batch cooling crystallization of ammonium oxalate in water, Journal of Crystal Growth, 342 (2012) 88-98.

[15] H. McLachlan, X. Ni, On the effect of added impurity on crystal purity of urea in an oscillatory baffled crystallizer and a stirred tank crystallizer, Journal of Crystal Growth, 442 (2016) 81-88.

[16] T. Togkalidou, M. Fujiwara, S. Patel, R.D. Braatz, Solute concentration prediction using chemometrics and ATR-FTIR spectroscopy, Journal of Crystal Growth, 231 (2001) 534–543.

[17] N.C.S. Kee, R.B.H. Tan, R.D. Braatz, Selective crystallization of the metastable α-Form of L-glutamic acid using concentration feedback control, Crystal Growth & Design, 9 (2009) 3044-3051.

[18] J. Cornel, C. Lindenberg, M. Mazzotti, Quantitative application of in situ ATR-FTIR and Raman spectroscopy in crystallization processes, Ind. Eng. Chem. Res., 47 (2008) 4870-4881.

[19] G. Zhou, A. Moment, S. Yaung, A. Cote, T.E. Hu, Evolution and application of an automated platform for the development of crystallization processes, Organic Process Research & Development, 17 (2013) 1320-1329.

[20] R.J. Davey, N. Blagden, G.D. Potts, R. Docherty, Polymorphism in molecular crystals: stabilization of a metastable form by conformational mimicry, J. Am. Chem. Soc.,

119 (1997) 1767-1772.

[21] X.Z. Wang, K.J. Roberts, C. Ma, Crystal growth measurement using 2D and 3D imaging and the perspectives for shape control, Chemical Engineering Science, 63 (2008) 1173-1184.

[22] F. Zhang, T. Liu, Y. Huo, R. Guan, X.Z. Wang, Investigation of the operating conditions to morphology evolution of β-l-glutamic acid during seeded cooling crystallization, Journal of Crystal Growth, (2016) http://dx.doi.org/10.1016/j.jcrysgro.2016.1009.1041.

[23] J. Nývlt, Kinetics of nucleation in solutions, Journal of Crystal Growth, 3 (1968) 377-383.

[24] C.Y. Ma, X.Z. Wang, Closed-loop control of crystal shape in cooling crystallization of L-glutamic acid, Journal of Process Control, 22 (2012) 72-81.

[25] J. Scholl, L. Vicum, M. Mazzotti, Precipitation of L-glutamic acid determination of nucleation kinetic, Chem. Eng. Technol., 29 (2006) 257-263.

[26] Y. Zhao, Y. Bao, J. Wang, S. Rohani, In situ focused beam reflectance measurement (FBRM), attenuated total reflectance Fourier transform infrared (ATR-FTIR) and Raman characterization of the polymorphic transformation of carbamazepine, Pharmaceutics, 4 (2012) 164-178.

[27] D. Duffy, M. Barrett, B. Glennon, Novel, calibration-free strategies for supersaturation control in antisolvent crystallization processes, Crystal Growth & Design, 13 (2013) 3321-3332.

[28] L. Helmdach, M.P. Feth, C. Minnich, J. Ulrich, Application of ATR-MIR spectroscopy in the pilot plant-Scope and limitations using the example of paracetamol crystallizations, Chemical Engineering and Processing: Process Intensification, 70 (2013) 184-197.

List of Table and Figure Captions

Table 1. Number of sampled spectra for establishing different calibration models

Table2. Characteristic wavenumbers for the functional groups of LGA solute

Table 3. Comparison of fitting criteria for different calibration models

Table 4. Comparison of model prediction performance

Figure 1. (a) Schematic of a crystallizer with monitoring instruments; (b) Experimental set-up for in-situ measurement

Figure 2. Experimental data distribution for establishing calibration models using ATR-FTIR

Figure 3. (a) IR spectra for different LGA solution concentrations at 46 °C; (b) Absorption peaks at the wavenumbers 1406 cm^{-1} and 1219 cm^{-1} for different LGA solution concentrations at 46 °C

Figure 4. IR spectra for LGA solution with 27.0 g/L concentration at different temperatures

Figure 5. Plot of model coefficients of M3 and the IR spectrum of LGA solution with 15.0g/L concentration at 25 °C

Figure 6. Absorption peaks with respect to the solution temperature for measuring three different solution concentrations: (I) 15 g/L; (II) 21 g/L; (III) 27 g/L

Figure 7. Real-time prediction results by using four calibration models at the solution concentration: (a) 12.0 g/L; (b) 23.0 g/L; (c) 35.0 g/L

Figure 8. Experiment on nucleation detection using different calibration models

Table 1. Number of sampled spectra for establishing different calibration models

Calibration models	Total spectra	Training spectra	Test spectra
M1	972	729	243
M2	640	480	160
M3	431	324	107
M4	497	373	124

Table 2. Characteristic wavenumbers for the functional groups of LGA solute

Wavenumber/cm^{-1}	Functional Groups
1730	C=O, stretching vibration of carboxylate, when pH<4.2, weak
1560	Asymmetric carboxylate ion stretching vibrations, high pH values, NH_2 deformation
1451	CH_2 deformation mode, no changes over pH area, weak
1406	Symmetric carboxylate ion stretching vibrations, high pH values
1219	C-O, stretching mode of carboxylate

**Table 3. Comparison of fitting criteria for four calibration models**

Regression	M1	M2	M3	M4
R^2 (training)	0.9991	0.9993	0.9994	0.9992
R^2 (test)	0.9991	0.9993	0.9993	0.9990
RMSEC	0.274	0.278	0.244	0.247
RMSEP	0.260	0.274	0.274	0.284

Table 4. Comparison of model prediction performance

Sampled zone		MSZ			USZ		
Concentration(g/L)		12.0	23.0	35.0	12.0	23.0	35.0
Number of spectra		19	18	18	18	19	19
Mean prediction	M1	12.23	23.20	34.89	12.27	23.34	34.71
(g/L)	M2	12.28	23.41	35.20	12.80	24.21	35.56
	M3	**11.84**	**23.09**	**35.04**	12.39	23.73	35.45
	M4	11.68	23.64	35.76	**12.15**	**23.25**	**34.77**
Averaged relative	M1	1.92	0.87	0.31	2.25	1.48	0.83
prediction error (%)	M2	2.33	1.78	0.57	6.67	5.26	1.60
	M3	**1.33**	**0.39**	**0.11**	3.25	3.17	1.29
	M4	2.58	2.78	2.17	**1.25**	**1.09**	**0.66**
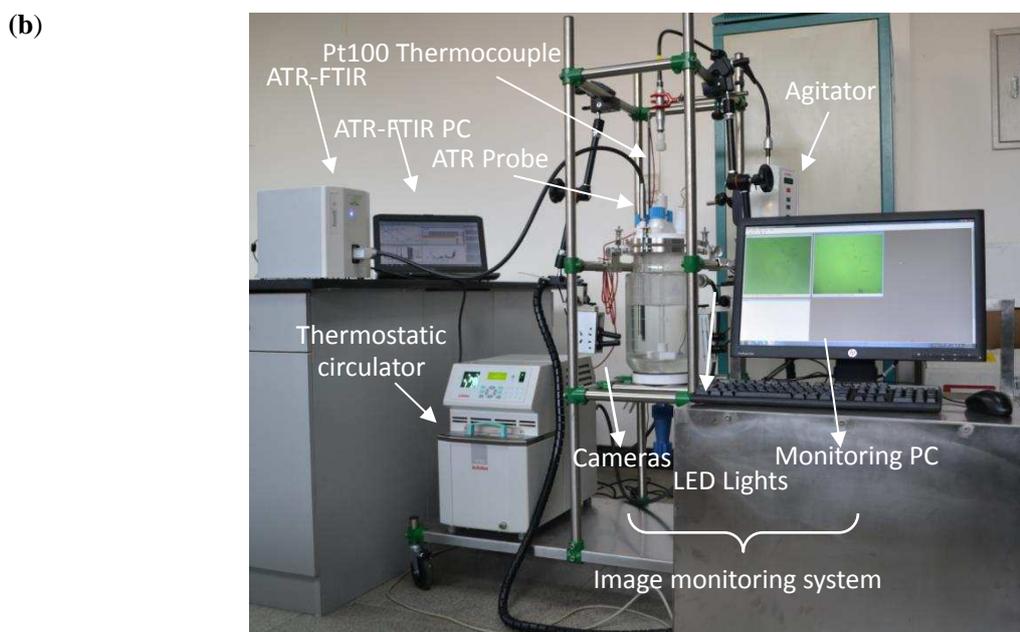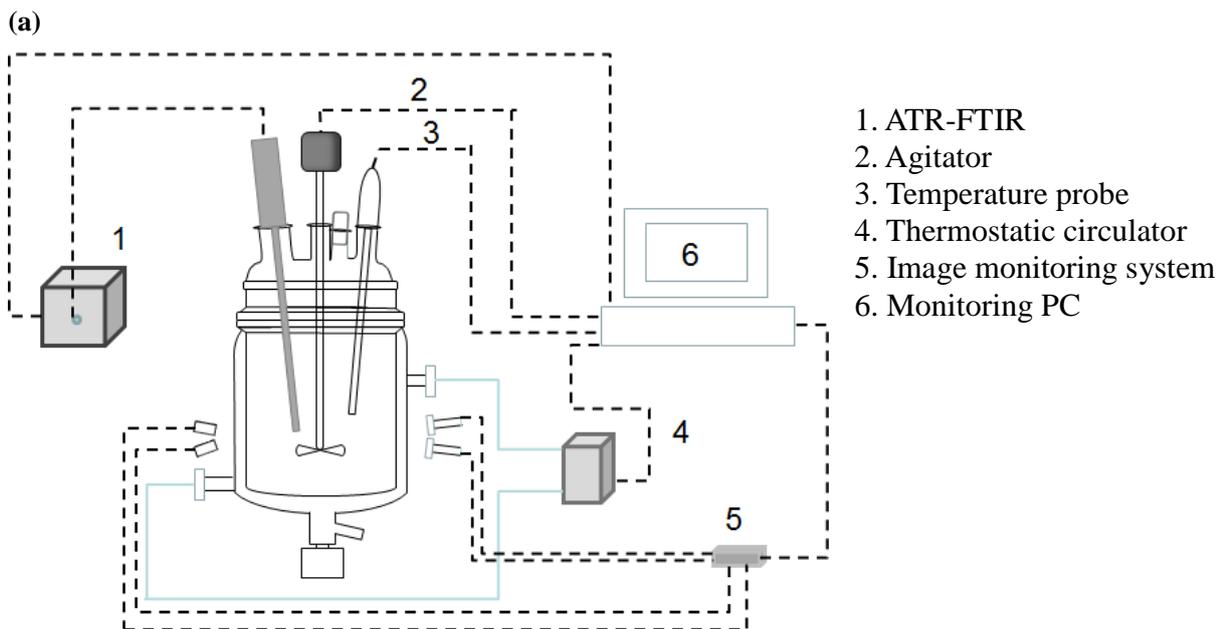
(a)

1. ATR-FTIR
2. Agitator
3. Temperature probe
4. Thermostatic circulator
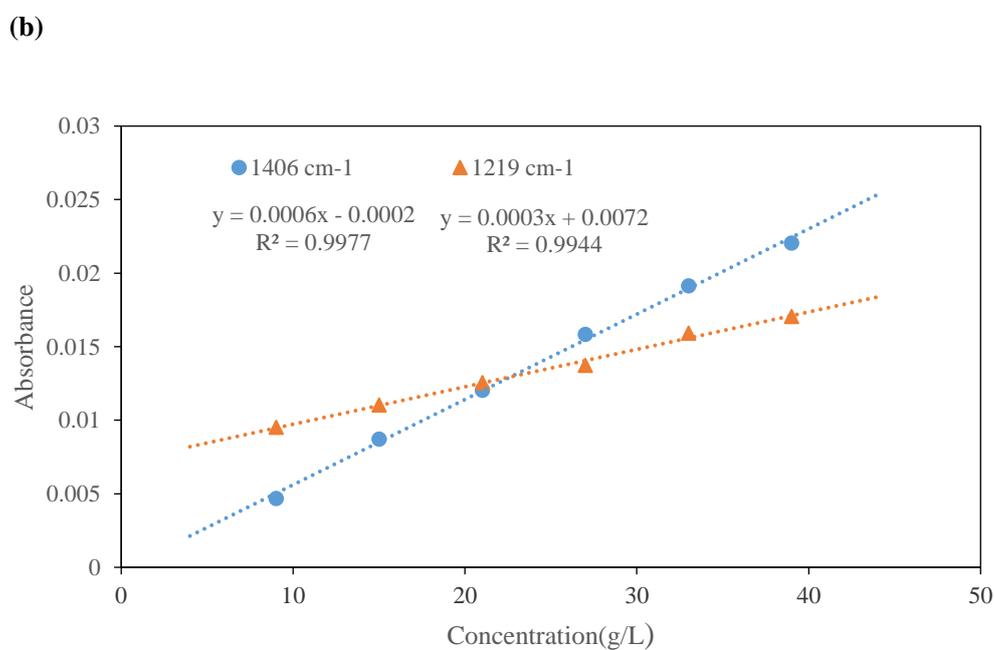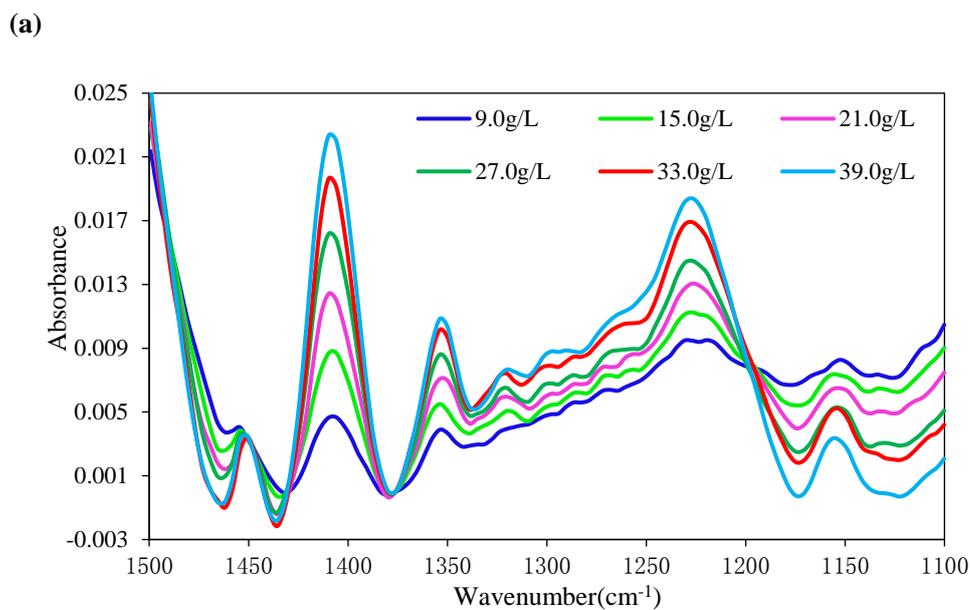5. Image monitoring system
6. Monitoring PC

(b)

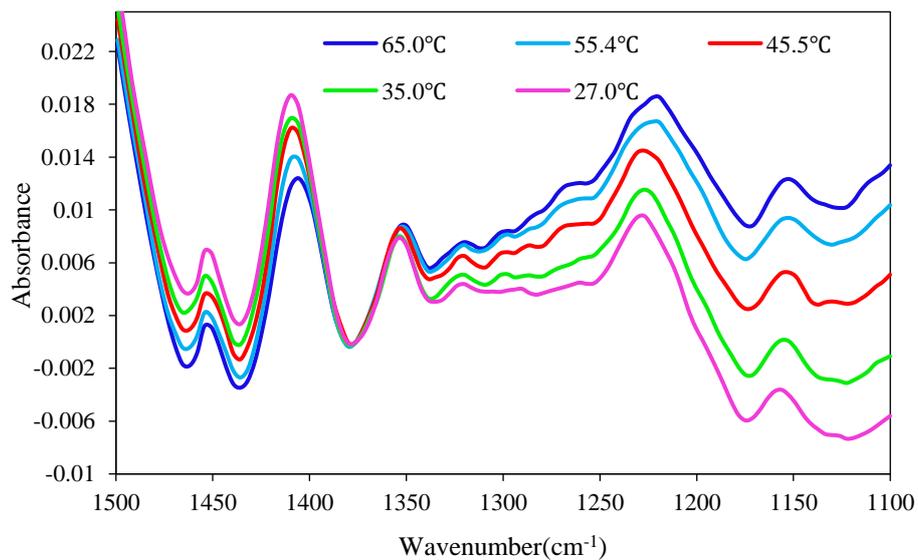**Figure 1. (a) Schematic of a crystallizer with monitoring instruments; (b) Experimental set-up for in-situ measurement**
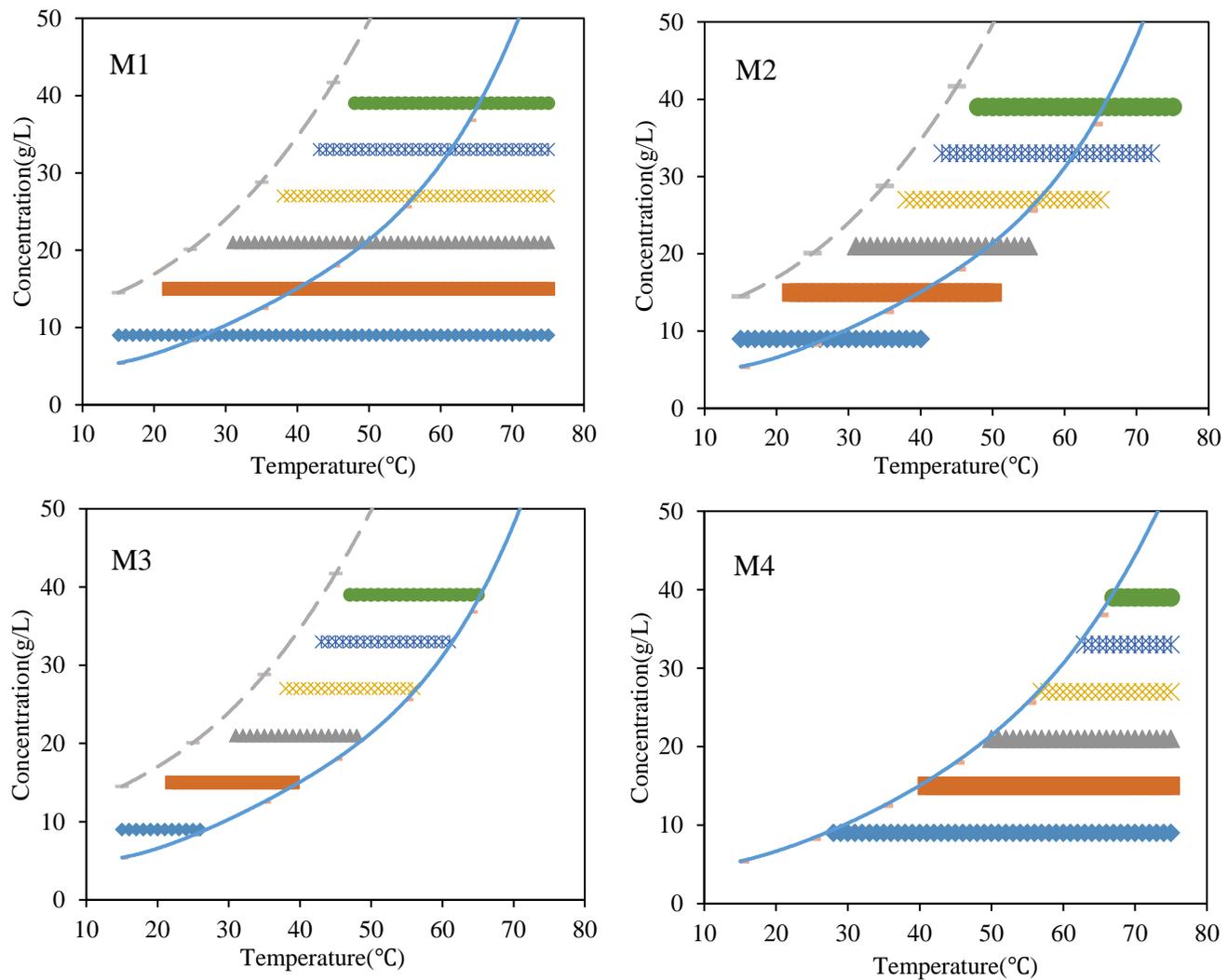
Figure 2. Distribution plot of sampled IR spectra for establishing calibration models
The blue solid curve indicates the solubility of β-form LGA, and the dashed gray curve indicates the
supersaturation of LGA under a cooling rate of 0.2℃/min.
**Legend: ◆ : 9.0g/L; ■ : 15.0g/L; ▲ : 21.0g/L; ✕ : 27.0g/L; ✳ : 33.0g/L; ● : 39.0g/L**

Figure 3. **(a) IR spectra for different LGA solution concentrations at 46 °C; (b) Absorption peaks at the wavenumbers 1406 cm⁻¹ and 1219 cm⁻¹ for different LGA solution concentrations at 46 °C**
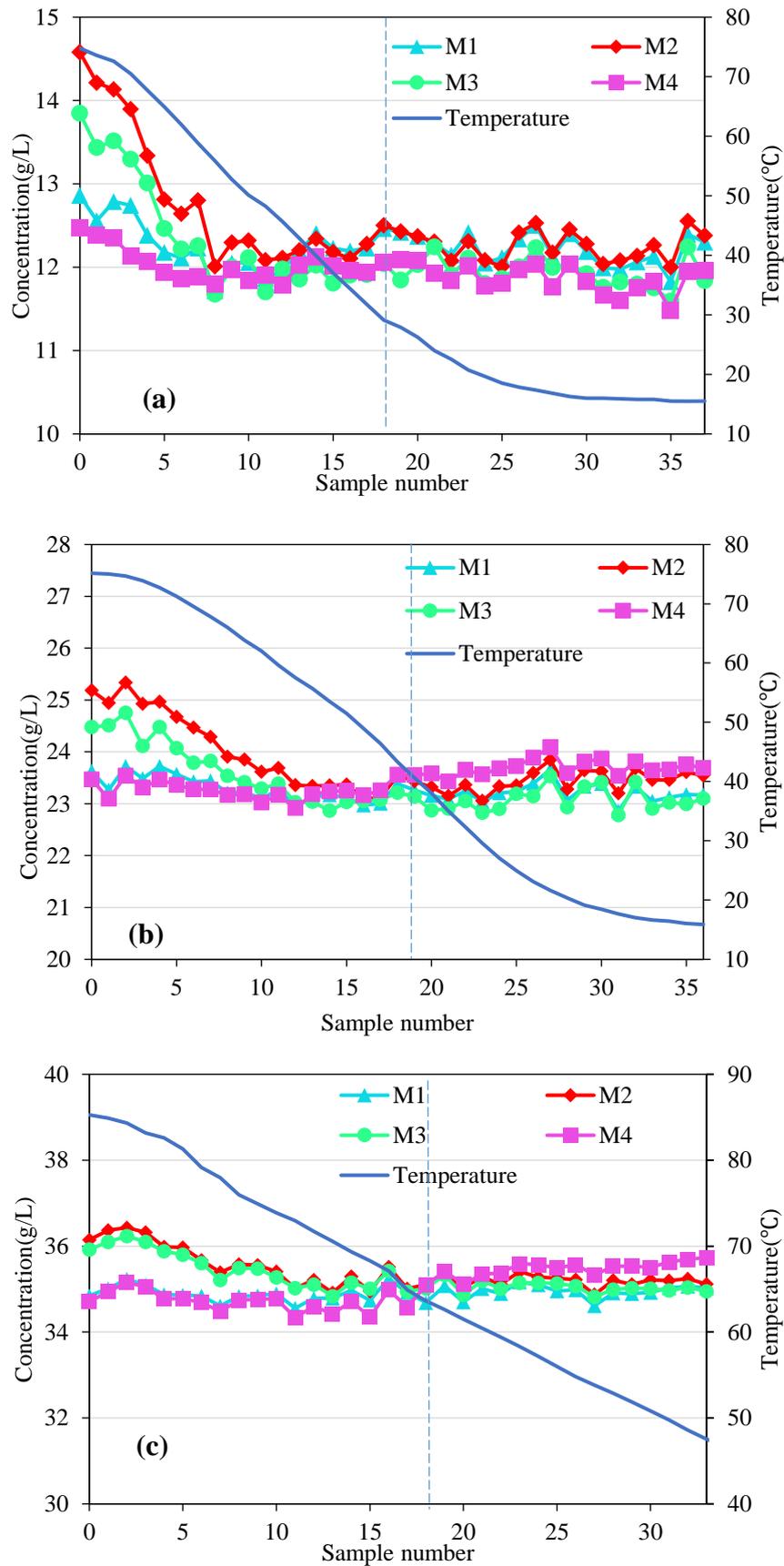
Figure 4. IR spectra for LGA solution with 27.0 g/L concentration at different temperatures
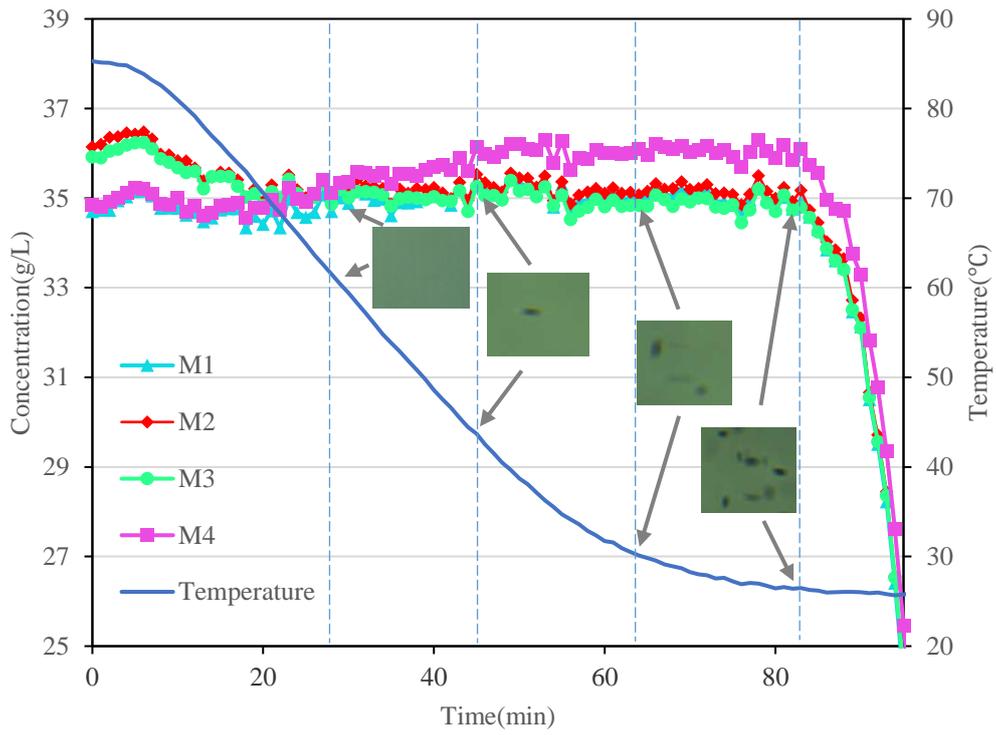

Figure 5. Plot of model coefficients of M3 and the IR spectrum of LGA solution with 15.0 g/L concentration at 25 °C
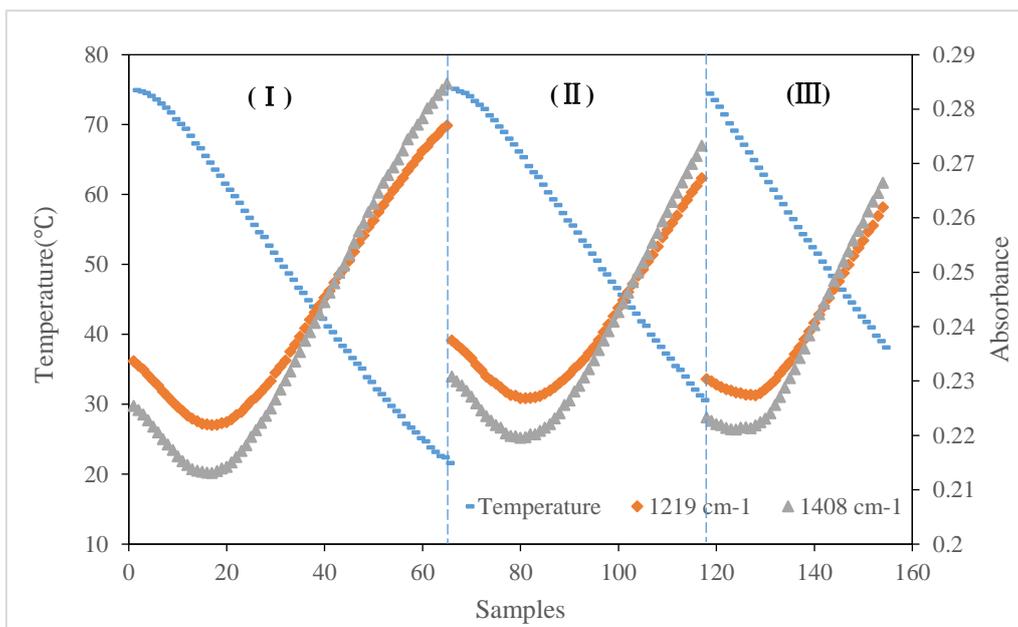
Figure 6. Absorption peaks with respect to the solution temperature for measuring three different solution concentrations: (I) 15 g/L; (II) 21 g/L; (III) 27 g/L.

Figure 7. Real-time prediction results by using four calibration models at the solution concentration: (a) 12.0 g/L; (b) 23.0 g/L; (c) 35.0 g/L. (Note: USZ is on the left and MSZ on the right of the dash line)

Figure 8. Experiment on nucleation detection using different calibration models